Sensors & Actuators: A. Physical 354 (2023) 114295

Contents lists available at ScienceDirect

Sensors and Actuators: A. Physical

journal homepage: www.journals.elsevier.com/sensors-and-actuators-a-physical

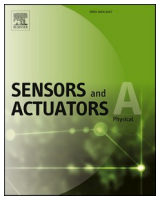

Batteryless NFC dosimeter tag for ionizing radiation based on commercial MOSFET

A. Pousibet-Garrido [a], P. Escobedo [a], D. Guirado [b,c], G.S. Ristic [d], A.J. Palma [a], M.A. Carvajal [a,*]

[a] ECsens, Department of Electronics and Computer Technology, Sport and Health University Research Institute (iMUDS-UGR), Research Centre for Information and Communications Technologies (CITIC-UGR), University of Granada, 18071 Granada, Spain
[b] Instituto de Investigación Biosanitaria, ibs.Granada. Hospital Universitario Clínico San Cecilio, Granada, Spain
[c] CIBER de Epidemiología y Salud Pública (CIBERESP), Granada, Spain
[d] Faculty of Electronic Engineering, University of Niš, Niš, Serbia

ARTICLE INFO

Keywords:
MOSFET dosimeter
NFC sensing tag
Batteryless
Smartphone

ABSTRACT

This paper reports the development, evaluation and validation of DosiTag, a dosimetric platform based on Near Field Communication (NFC) technology. The designed system comprises two main parts: a passive NFC sensing tag as the dosimeter unit, which includes a commercial P-channel MOSFET transistor as radiation sensor; and an NFC-enabled smartphone running a custom-developed application as the reader unit. Additionally, a cloud service based on the messaging protocol Message Queue Telemetry Transport (MQTT) has been implemented using a broker/client architecture to allow the storage and classification of the patient's data. The dosimeter tag was designed using commercial low-power integrated circuits (ICs) and it can operate without any external power supply or battery, being supplied by the smartphone through the radio frequency (RF) energy harvested from the NFC link. The radiation dose is measured through the increase of the DMOS transistor source voltage using the smartphone as the reader unit. Two tag prototypes have been characterized with a 6 MV photon beam and radiation doses up to 57 Gy and 42 Gy, respectively. The achieved average sensitivity is (4.37 ± 0.04) mV/Gy with a resolution of 2 cGy, which goes beyond the state-of-the-art of previous NFC dosimeters and places DosiTag as a low-cost promising electronic platform for dose control in radiotherapy treatments.

1. Introduction

In an effort to improve the quality of the medical use of ionizing radiation, in vivo dosimetry (IVD) emerged as a direct method of measuring the radiation doses received by patients during their radiotherapy sessions. The use of IVD has become more widespread since the World Health Organization (WHO) and other entities considered it an effective way of checking the quality of the entire radiotherapy process [1,2]. Current solutions for such dose measurements are based on detectors like diodes, thermoluminescent dosimeters (TLDs), metal oxide semiconductor field-effect transistors (MOSFETs), film badges or optically stimulated luminescence dosimeters (OSLDs) [3]. In the case of MOSFETs, the p-type devices generate during irradiation electron-hole pairs proportional to the delivered dose, which can be later read using an appropriate metering system [4]. Their advantages include good linearity, very compact size, immediate readout and easy calibration, thus becoming increasingly popular both commercially [5,6] and in research [7–9]. To further improve the sensitivity, transistors with thick gate oxides specially designed for radiation detection have been manufactured, known as RADFETs (Radiation-Sensitive Field Effect Transistors) [10–12]. However, for radiation doses used during typical radiotherapy sessions, the possibility of using commercial MOSFETs as dosimeters instead of RADFETs can greatly reduce the cost of the dosimetry system [13]. Nevertheless, achieving such a dosimetry system with commercial MOSFETs [14–17] requires a reader unit implementing the necessary signal conditioning stages in terms of amplification, filtering and compensation of the temperature effect [7,13,18]. The reader units for these dosimetric systems are usually desktop-based devices [7], which require the use of cables connected to the sensor modules placed on the patient, thus making the process cumbersome and uncomfortable for the patient. To make the system more comfortable for the patient and user-friendly for the healthcare personnel, wireless RFID or NFC-based systems have been proposed [7, 19–21]. With this approach, only the NFC dosimetric sensing tag and a

* Corresponding author.
E-mail address: carvajal@ugr.es (M.A. Carvajal).

https://doi.org/10.1016/j.sna.2023.114295
Received 26 October 2022; Received in revised form 14 February 2023; Accepted 5 March 2023
Available online 7 March 2023

smartphone with a custom application are required.

A smartphone can be currently purchased for a relatively low price and developing a custom smartphone application is feasible with the completely accessible integrated development environments (IDE's) provided by the main mobile software distributors (Android and iOS). Therefore, the implementation of this type of systems is a very cost-effective solution with great potential for market access [22]. In addition, if NFC technology [23] is used and the tag's power consumption is sufficiently low, no batteries are required and consequently the cost, maintenance and complexity of the system will greatly decrease. For this reason, several examples of NFC sensing tags can be found in the literature [24–27]. Since the power consumption of the MOSFET-based dosimeters is usually low [7–29], it is possible to implement a battery-less NFC dosimeter.

In this work, we present the development, characterization and validation in hospital facilities of DosiTag, an enhanced NFC-based dosimeter for ionizing radiation with wireless power and communication. The system is composed of a credit-card size NFC tag that incorporates a MOSFET-based sensor module and a smartphone to supply the system and read out the dose measurements. The presented system is an enhanced and redesigned version of a previous NFC-based dosimeter from our research group [7], where a number of novelties and improvements have been implemented. Firstly, the inclusion of a microcontroller unit (MCU) allows the full control of the measurement variables (e.g., measurement time, start/end control, etc.), the possibility to endow the pins with new and diverse functionalities (e.g., turn on/off the sensor module) as well as the use of several Analog-to-Digital Converter (ADC) modules and the full implementation of bidirectional communication between the microcontroller and the smartphone. Secondly, a new amplification stage has been designed to increase the system resolution. Additionally, the new version allows the irradiation of the complete dosimeter tag, not only the sensor module, and the total irradiation dose has been increased. The new compact design allows the possibility of tag encapsulation, so that the dosimeter tag can be sterilized or submerged in liquids. Regarding the reader unit, a new smartphone app has been developed from scratch and Internet-of-Things (IoT) capabilities have been included thanks to the implementation of a cloud service based on MQTT protocol [30–33] which allows storage, distribution, and classification of the patient's data.

2. Materials and methods

2.1. Experimental

2.1.1. Simulation, fabrication, and characterization tools

For thermal characterization of the radiation sensor, the device was entered into a climatic test chamber VCL4006 (Vötoshch Industrietechnik, Germany) and the electrical characterization was conducted using a custom-developed reader based on 12-bit ADC model MCP3208 (Microchip, Chandler, Arizona, USA). Numerical simulations for the optimization of the tag antenna design were conducted using ADS, i.e., Advanced Design Simulator software (Keysight Technologies, Santa Clara, CA, USA). The final prototype of the PCB (Printed Circuit Board) was fabricated on 1.5-mm FR-4 substrate. For NFC antenna characterization, the precision impedance analyzer model Agilent 4294 A (Keysight Technologies, Santa Clara, California, USA) was employed. Android Studio 2021.1.1 was the IDE employed to program the custom smartphone application. The app was designed and validated with Android 10 QKQ1 (API level 29). However, the app supports diverse Android versions since the lowest API level supported is 21 (Android 5.0). The smartphone model used as the NFC reader was the Xiaomi Redmi Note 9 Pro (Xiaomi, Beijing, China).

2.1.2. Sample preparation and irradiation setup

A Linear Accelerator (LINAC) Siemens Artiste (SiemensAG, Germany) was employed to irradiate two replicas of the prototype based on the commercial p-type MOSFET ZVP3306 (Diode Inc., Plano, TX, USA). The total area of each tag was irradiated in sessions of 3 Gy with a 20 × 20 cm^2 field and 6 MV photon beams. The isocenter of the irradiation source was placed on the zone of the tag where the pMOSFET sensor is located. To measure in electronic equilibrium condition in the sensor, a 1.5-cm thick solid water layer was located on top of the PCBs, and 5 cm thick solid water was placed below it. For this purpose, a 3D-printed holder for the boards was designed and fabricated with PLA using a 3D printer model Creality cr-x (Shenzhen Creality 3D Technology Co., Ltd, Shenzhen, China). With this methodology, a total dose of 57 Gy was irradiated for the first tag and 42 Gy for the second tag.

To test and evaluate the response of the DosiTag, the obtained results have been compared with our previously developed NFC dosimeter [7] as well as with our desktop dose reader [34] using the same pMOSFET as radiation sensor. As usual in this kind of sensors, to evaluate the increment of the threshold voltage shift, a constant current drain and a diode configuration (drain short-circuited with the gate) were used to measure this increment on the source terminal of the transistor [8,10,35–38].

2.2. DosiTag design

2.2.1. System architecture

The functional block diagram of the dosimetric system is depicted in Fig. 1a, including all the functional blocks of the NFC tag; the wireless connection to the smartphone through the NFC link for RF power supply and communication; and the IoT integration by means of the cloud architecture based on the MQTT broker/client protocol. As shown in Fig. 1a, the NFC sensing tag consists of an RFID chip and antenna, an ultra-low power MCU to acquire the measurements, a voltage regulator to provide a regulated voltage reference for the ADC of the microcontroller, a charge pump to double this voltage as supply voltage, a current source, conditioning circuitry, a temperature sensor, an instrumentation amplifier (IA) to increase the resolution of the system, and the radiation sensor module, composed of a pMOSFET and a JFET. The different components of the tag and the IoT integration will be explained in the next subsections. On the other hand, Fig. 1b shows a photograph of the final DosiTag prototype (dimensions of 76 ×40 mm^2) with the physical functional blocks.

2.2.2. RFID chip and antenna

The NFC chip M24LR64E (STMicroelectronics, Geneva, Switzerland) along with an ad-hoc designed planar antenna was used as energy harvester to enable the development of battery-less design, data storage, and communication between the MCU and the smartphone [39]. This NFC chip operates in the High Frequency band (HF, 13.56 MHz) and it includes an I^2C serial communication port. Since this RFID chip does not directly provide a regulated voltage in the energy harvesting mode, a low dropout voltage regulator (LDO) (2.5 V regulator MCP1824T-2502E, Microchip, Chandler, Arizona) was included to supply the system. When correctly coupled to the reader (i.e., the user's smartphone), the NFC chip is able to provide a maximum current that is selectable (300 μA, 1, 3, or 7 mA) according to the harvested electromagnetic (EM) field, which is enough to power the additional circuitry. In the case that the EM field is not sufficient to provide the required power, the chip cuts off the output voltage so that the system does not turn on. This is an advantage in terms of repeatability since the delivered power to the system will be always the same as long as the coils of the tag and the smartphone are correctly overlapped.

The custom-designed tag antenna is a planar coil based upon the internal capacitance of the M24LR64E NFC chip (Fig. 1b). This antenna has a dual purpose, since it is used to establish bidirectional communication with the smartphone and also to harvest the RF energy to supply the tag. The internal tuning capacitor of the NFC chip has a value of 27.5 pF at 13.56 MHz. Therefore, we require a coil of 5.01 μH to get a parallel LC resonant circuit at the desired HF frequency. The final dimensions and number of turns obtained after numerical simulations

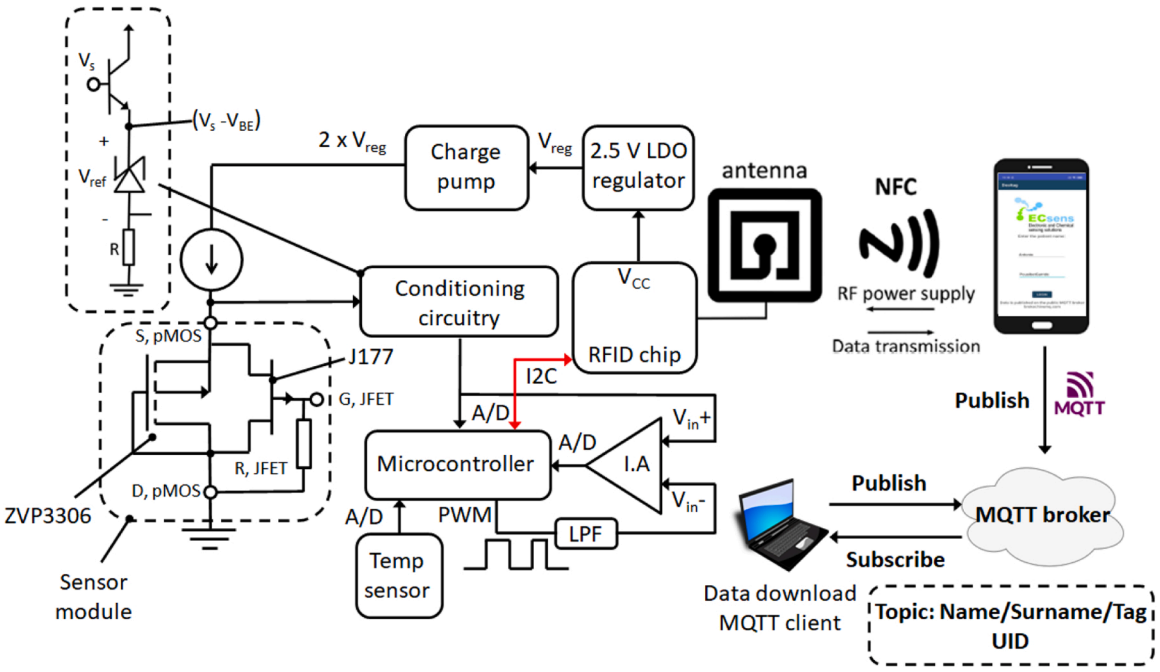

(a)

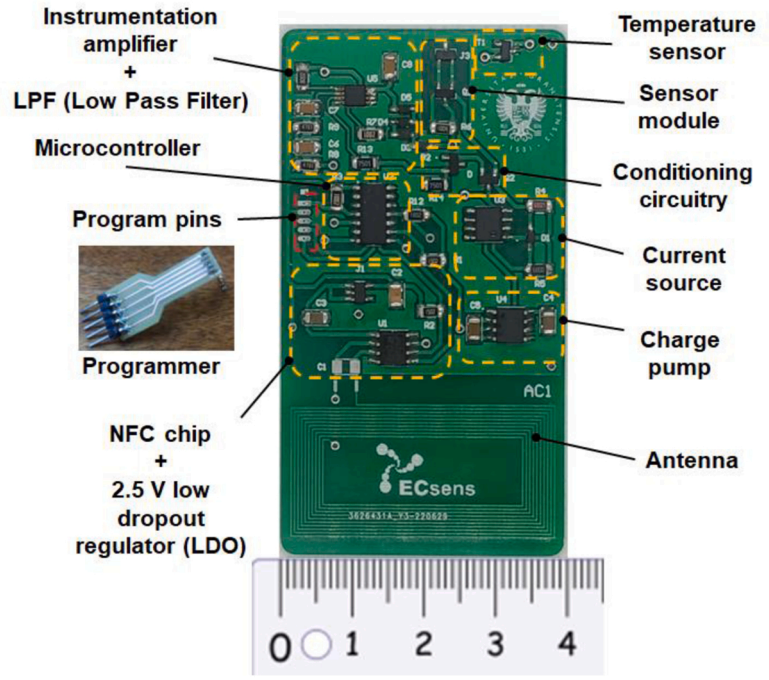

(b)

Fig. 1. (a) Block diagram of the NFC tag including the radiation sensor module; (b) Photograph of the fabricated NFC tag with the functional blocks and dimensions.

were 38 mm × 19 mm and N = 10 turns, being 250 μm both the inter-spacing between the conductor lines and their width.

2.2.3. *Microcontroller unit*

An ultra-low power microcontroller PIC16LF1703 (Microchip, Chandler, Arizona) is used to acquire the measurements from the different sensors, storing the data in the EEPROM memory of the NFC chip through the I^2C port. The microcontroller uses three ADCs for this task, whose range is the same than the supply voltage range, i.e., from 0 up to 2.5 V. Firstly, after setting the cut off frequency of the Low Pass Filter (LPF) in the amplification stage, the direct pMOSFET source voltage is measured, and subsequently the amplified source voltage is measured. For this purpose, conditioning circuitry was designed to adapt the source voltage of the sensor to the common-mode rejection

ratio of an ultra-low power rail-to-rail instrumentation amplifier INA321 (Texas Instruments, Dallas, TX, USA). A Pulse Waveform Modulation (PWM) signal is generated with the Capture/Compare/PWM (CCP) module of the MCU, which is low-pass filtered (see Fig. 1a) to assure a constant voltage, restart the measurement and prevent the output voltage from trespassing the ADC range limits [28]. Finally, since MOSFET threshold voltage is highly temperature-dependent, the temperature sensor MCP9701A (Microchip, Chandler, Arizona) was included in the tag design to monitor the temperature with a resolution of 0.125 °C, which is used for thermal compensation (see Section 3.2).

2.2.4. Signal conditioning and power management

The most straightforward way to measure the threshold voltage shift of the transistor is to bias it at constant drain current and to set up the pMOSFET in diode configuration (short-circuiting drain and gate) [36, 13,28]. For this purpose, the tag conditioning circuit includes a current source and a buffer to avoid the loading from the conditioning circuitry. The implementation of the current source was conducted using the temperature-compensated circuit LM334 from Texas Instruments (Dallas, TX, USA) using the topology suggested by the manufacturer to reduce the output current thermal drift [7]. The buffer is a general-purpose bipolar transistor BC848C (Infineon AG, Germany), whose role is to prevent the subtraction of the drain current by the emitter resistor and the ADC, and it is also used for thermal drift correction, as shown in the previous work [7]. The selected collector current is dependent on the value of the collector resistor, the source voltage (V_s) and the selected drain current, all of which will be described in the next subsections for the pMOSFET ZVP3306. The output voltage of the conditioning circuit must be between 0 and 2.5 V to accommodate the ADC input voltage range. However, to take advantage of the Common Mode Rejection Ratio (CMRR) of the INA321 instrumentation amplifier and to achieve constant gain, the output must lie approximately between 0.8 and 1.5 V. Thus, a reference voltage (V_{ref}) was included to decrease the voltage value before the ADC input and the V_{in+} of the IA. In accordance with the conditioning circuitry shown in Fig. 1a, the ADC input voltage and the instrumentation amplifier is given by Eq. (1):

$$V_{in}^{ADC\_IA} = V_S - V_{BE} - V_{ref} \quad (1)$$

where V_S (sensor source voltage), V_{BE}(bipolar transistor base-emitter voltage), and V_{ref} voltages are shown in Fig. 1a. The chosen reference voltage was the model LM385–1.2 from Texas Instruments, which is capable of providing a stable voltage of 1.23 V with a thermal drift of typically 20 ppm/°C. The major constraint is that the reverse current needs to lie in the range from 10 μA to 20 mA. Considering that the collector voltage of the buffer was around 2.1 V at the selected bias current of the ZVP3306, that is, approximately 0.9 V after the V_{ref}, a 7.5 kΩ collector resistor was included to ensure a reverse current of 120 μA, which lies within the adequate range of this reference voltage.

On other hand, the instrumentation amplifier INA321 was included to increase the accuracy and resolution of the system. The inverter input (V_{in-}) is controlled by a PWM signal generated by the microcontroller and doubly low-pass filtered to ensure a constant voltage in the input [36,40]. The voltage after the conditioning circuitry is directly measured by the ADC of the microcontroller and is the non-inverter input (V_{in+}) of the IA (see Fig. 1a). The signal is amplified by a gain of 45 and measured by other ADC input of the MCU. Thus, the resolution was considerably increased, obtaining 2.44 mV/count in the direct voltage source ADC channel and 0.05 mV/count in the amplified ADC channel (see Fig. 1a). It is worth mentioning that a voltage ripple below 1 mV was obtained at the output of the INA321, which is lower than the accuracy of the ADC, so it does not affect the measurement.

The energy harvested by the tag antenna is firstly rectified by the NFC chip and then regulated using the voltage regulator. The resulting power is finally used to supply the DC-DC voltage pump, which is based on the ADM660 IC (Analog Devices, USA). This IC was selected because of its low quiescent current of only 600 μA, and because its implementation only requires two external capacitors, thus implying a reduced number of components in the PCB and easier implementation. Thus, the regulated voltage of 2.5 V is augmented up to 5 V in order to achieve a higher maximum value of the drain-to-source voltage. Assuming the ADM660 has the efficiency of a usual DC-DC converter (80 %) and taking into account the quiescent current of 600 μA and the voltage regulator MCP1824T-2502 quiescent current (120 μA), a total power around 3.3 mW must be provided by the M24LR64E IC.

Finally, to supply the INA321 in the voltage range specified by the manufacturer (2.7–5.5 V), four 1N4148 diodes (Onsemi, Phoenix, Arizona) were used to reduce the voltage from the charge pump down to 3 V. In this way, when the instrumentation amplifier is saturated at high voltage, it does not exceed the input span of the microcontroller ADC.

2.2.5. Sensor module

The radiation sensor is based on the general-purpose DMOS transistor model ZVP3306, which we had already tested and evaluated with our desk reader unit [40]. The module sensor also includes a P-channel JFET that avoids the potential damage during the storage and irradiation process caused by electrostatic discharge (Fig. 1a) by connecting the drain and source terminals of the pMOSFET. This configuration was validated in the previous NFC-based dosimeter [7] with the J175 JFET (Eindhoven, Netherlands), similar to the sensor module for the desk reader [36], where an N-channel JFET was used. However, for this work the J177 (NXP Semiconductors, Eindhoven, Netherlands) was chosen. In the present work, the gate was directly connected to the charge pump supply voltage, which was sufficient to disconnect the JFET. Finally, during the storage and irradiation period, the voltage in the gate of the JFET is 0 V, so the transistor is ON and prevents the electrostatic discharges in the pMOSFET sensor. Moreover, this sensor module can be controlled by an output pin of the microcontroller to perform several measurements without the need to power the board multiple times.

2.3. Software design

2.3.1. Smartphone application

The NFC chip M24LR64E-R is compliant with the Android NFC-V standard and compatible with the ISO15693 RFID specification. On this basis, the smartphone application was built on the ISO15693 specification and uses specific NFC commands to communicate and control the device. The commands can be executed via RF by the smartphone or via I^2C by a microcontroller. Fig. 2a, b show some screenshots of the application user interface. Before approaching the smartphone to the DosiTag, the user has to fill several fields of personal data related to the patient, as shown in Fig. 2a. Then, the next screen is shown (Fig. 2b), which is composed of text fields that show information such as the tag UID, ambient temperature, date of the measurement, duty cycle of the PWM for the IA, and direct and amplified voltage shift of the pMOSFET source.

The user can now approach the smartphone to the DosiTag to trigger the NFC link. At this point, the system is powered by the EM field harvested from the smartphone and one second later the measurements of the temperature and the direct and amplified source voltage are taken by the microcontroller. 1024 measurements are taken at the maximum sample frequency of the ADC, averaged by the microcontroller and recorded in the NFC EEPROM to be subsequently sent to the smartphone. The delay of one second is necessary for the system to correctly stabilize so that the measurements are always taken at the same time. This is an important issue because an initial decay of the source voltage takes place when a pMOSFET is biased due to the activation of the interface state. We can minimize the effect of this decay by always using the same time during which the pMOSFET is biased prior to conducting the source voltage measurements. The acquired ADC measurements are read and displayed by the smartphone when the user presses the “READ”

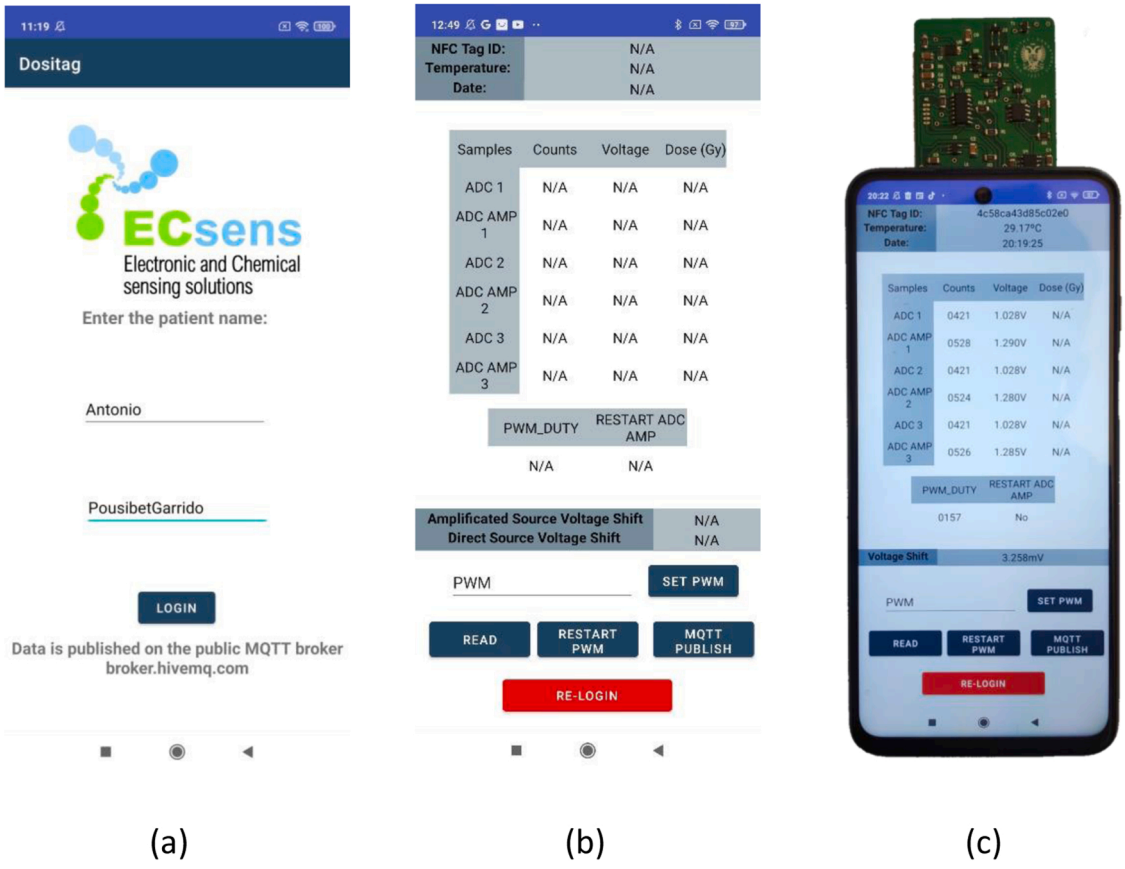

Fig. 2. (a-b) Screenshots of the custom-designed Android application; (c) Experimental setup for NFC measurements.

button. This process must be repeated two times, before and after the irradiation, to calculate the increment of the voltage source. Finally, the source voltage shift is displayed on the screen. Once this process has been completed, the user can publish the final value of the voltage source shift in the MQTT broker to be read by another MQTT client to store and graph each patient's data.

3. Results and discussion

3.1. NFC antenna performance

The fabricated planar coil was characterized over the frequency before and after attaching the NFC chip. In the first case, the obtained inductance value and quality factor (Q) of the coil is shown in Fig. 3a. The inductance value at 13.56 MHz is 4.86 μH, which is very close to the desired inductance of 5.01 μH. The achieved quality factor is higher than 50, adequate for an efficient energy harvesting. The LC resonant circuit

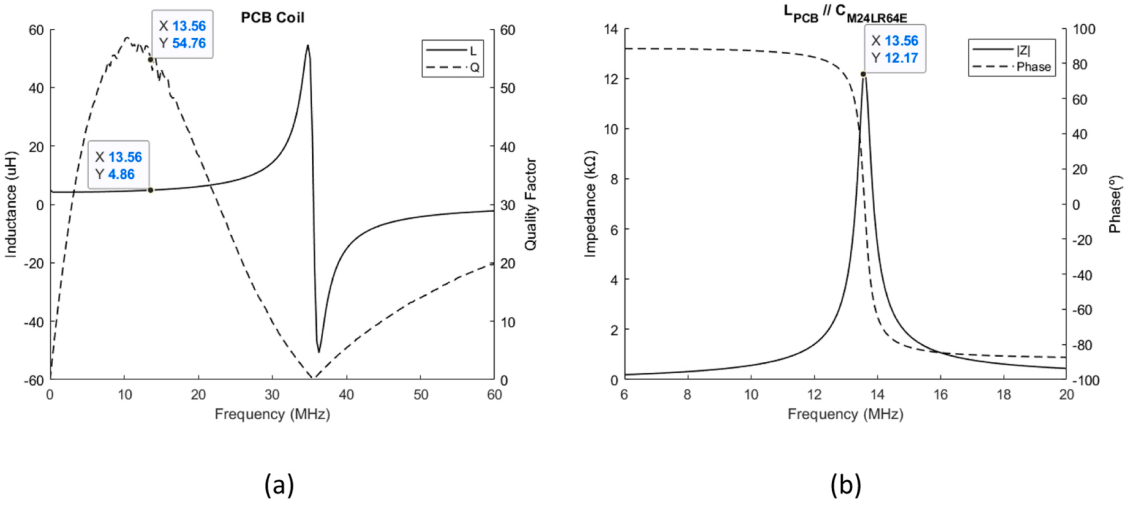

Fig. 3. (a) Measured inductance (L) and quality factor (Q) of the fabricated planar coil without the M24LR64E NFC chip; (b) Measured impedance and phase of the antenna with de M24LR64E chip attached.

is completed once the M24LR64E NFC chip is attached to the PCB. Consequently, a new frequency sweep was conducted to measure both the phase and impedance of the resonant circuit. As can be observed in Fig. 3b, the antenna resonates at a frequency of 13.62 MHz, close enough to the designed frequency of 13.56 MHz so that a parallel tuning capacitor was not necessary to adjust the frequency of resonance.

3.2. Thermal dependence

The designed circuitry for thermal compensation and conditioning is similar to the one shown in our previous NFC dosimeter unit [7] (see Fig. 1a). As in the previous work, to bias the device for reading out and reducing the thermal coefficient of the drain voltage, the BJT collector and pMOSFET drain currents were properly selected. A linear model is assumed for the thermal behavior as already assumed in previous works with good results [7]. Therefore, the thermal voltage drift can be expressed as follows:

$$\Delta V_{in}^{ADC} = \alpha \Delta T, \Delta V_{in}^{ADC\_AMP} = G \bullet \alpha \Delta T, \Delta V_S = \alpha_S \Delta T, \Delta V_{BE} = \alpha_{BE} \Delta T \quad (2)$$

where α is the thermal coefficient of the direct input voltage of the ADC, $G \bullet \alpha$ is the thermal coefficient of the amplified ADC input voltage, α_S is the thermal coefficient of the pMOSFET source voltage, and α_{BE} is the linear temperature coefficient of the BJT base-emitter voltage. Since the thermal drift of the voltage reference is small, it can be neglected, so the thermal drift in the ADC voltage is given by the following Eq. (3):

$$\alpha = \alpha_S - \alpha_{BE} \quad (3)$$

Therefore, if α_S and α_{BE} are very close, the thermal coefficient of the input voltage of the ADC is greatly minimized. In a previous work [40], we characterized the thermal drift of the ZVP3306 for multiple currents. With these results, in the previous NFC reader [7] we used a current value of 220 μA for the ZVP3306 in the saturation region with the gate and source short-circuited, and collector current of the buffer of 30 μA to improve the thermal dependence. However, for this DosiTag, it has been necessary to readjust these currents due to the addition of the IA and the MCU. Finally, to improve the thermal dependence, we used a drain current of 190 μA for the ZVP3306 in the saturation region with the gate and source short-circuited, obtaining a thermal coefficient of $\alpha_S = (-2.20 \pm 0.12)\text{mV}/^\circ\text{C}$ and a collector current for the buffer of 120 μA, so the thermal coefficient was $\alpha_{BE} = (-2.21 \pm 0.01)\text{mV}/^\circ\text{C}$. It should be noted that the temperature dependence of the LM334 current source was measured in the previous work [7] with a 12 kΩ resistor, a resistance that is equivalent to the ZVP3306 at 220 μA. The experiment concluded with a very low thermal drift of 70 nA/°C.

To conduct the DosiTag thermal dependence characterization, the tag was powered up using a DC power source at 5 V and it was located inside the climate chamber, where the temperature was swept from 10 up to 50 °C in increments of 5 °C. The source voltage of the pMOSFET transistor (V_S), the amplified source voltage of the pMOSFET transistor (V_{S_AMP}), and the emitter voltage of the bipolar transistor (V_E) were measured and the corresponding linear temperature coefficients were calculated. The direct thermal coefficient was reduced from $\alpha_S = (-1.76 \pm 0.33)\text{mV}/^\circ\text{C}$ down to $(0.45 \pm 0.08)\text{mV}/^\circ\text{C}$, which is in good agreement with our previous work [7]. If we normalize dividing by the gain the output signal of the IA, the thermal coefficient results in $\alpha = (0.32 \pm 0.05)\text{mV}/^\circ\text{C}$, which is considerably lower than the direct thermal coefficient of the previous NFC dosimeter. The reduction of the thermal coefficient in the amplified channel is mainly due to the IA having a negative thermal dependence. Finally, a reduction of 75 % in the direct thermal coefficient and 82% in the amplified normalized thermal coefficient was obtained.

3.3. Irradiation measurements

Two replicas of the developed DosiTag system were irradiated using the experimental setup described in Section 2.1.2. The first one was used to check the durability and the resistance of the electronics against the ionizing radiation, and only measured the direct source voltage of the pMOSFET. It was experimentally checked that the system was still working properly after an irradiated dose of 57 Gy. In the second prototype, the instrumentation amplifier was employed to improve the accuracy and the resolution of the dosimeter. In both cases, the source voltage was measured three minutes after each irradiation to minimize short-term fading effect. Therefore, this DosiTag has been designed in order to have one channel with lower resolution for the measurement of high doses (e.g., 10 Gy) and a channel with much higher resolution for the measurement of low doses (e.g., 3 Gy) so that the increase of the amplified source voltage does not exceed 0.7 V (see Section 2.2.4) as this is the range where the ADC and IA operate with higher linearity. As shown in Fig. 4, very good linearity was obtained in the increase of both the direct and amplified normalized source voltage as a function of the received dose.

The obtained average sensitivity of the low-resolution channel (LRC) of the DosiTag unit was (4.35 ± 0.17) mV/Gy, while the sensitivity of the high-resolution channel (HRC) was (4.37 ± 0.04) mV/Gy with a resolution of 79 cGy and 2 cGy, respectively. The achieved results are in good agreement with the average sensitivity measured in previous studies of the DMOS transistor ZVP3306 [13,41] including the previous NFC dosimeter [7], which was (4.75 ± 0.15) mV/Gy with a resolution of 17 cGy. This means that we have achieved an improvement of the resolution by a factor of 8. Finally, it should be noted that each sample plotted on the Fig. 4 is the mean of three measurements taken after each irradiation.

Source voltage recovery after irradiation was studied using a new sample of the system. This prototype was irradiated in three batches of 3 Gy, and after the last irradiation, the source voltage was measured every 10 min for two hours. According to Fig. 5, the source voltage decays with an average slope of (−6.3 ± 0.4) μV/min, which is in agreement with a previous study [42]. This recovery implies a dose underestimation of (−1.62 ± 0.06) mGy/min. Therefore, the error due to source voltage recovery can be considered negligible if the measurement is performed in the first 10 min after irradiation.

To evaluate the response of the DosiTag at low doses and to determine the system resolution, a set of 4 irradiation sessions of 50 mGy was performed. A thermal correction was applied using the thermal coefficient obtained in Section 3.2 and the temperature measured with the temperature sensor included in the prototype. In the last session (0.2 Gy in Fig. 6), the DosiTag was cooled by 1.7 °C before irradiation to study the thermal correction during irradiation. The obtained results are shown in Fig. 6, where thermal correction reduced the error due to the thermal shift in the last irradiation session, thus allowing the system to detect irradiation doses of 5 cGy.

3.4. Advantages and limitations of the system

As previously stated, DosiTag is an enhanced design of an earlier version of NFC dosimeter developed in our research group [7]. As a summary, Table 1 shows the main improvements and/or novelties of DosiTag system compared to the previous version. Apart from these advantages, the system also presents some limitations that deserves a mention. In particular, the inclusion of the amplification stage entails the inconvenience of the establishment time of the low pass filter for fixing the inverting input to the desired voltage. Therefore, the system must wait a minimum of one second before making the measurement. On the other hand, a correct alignment between the tag and the smartphone coils is required so that enough energy is harvested to power the system up. This means that the smartphone must be held in the correct position (i.e., correctly aligned with the tag and at a short distance) for at least one second while it is placed on the patient.

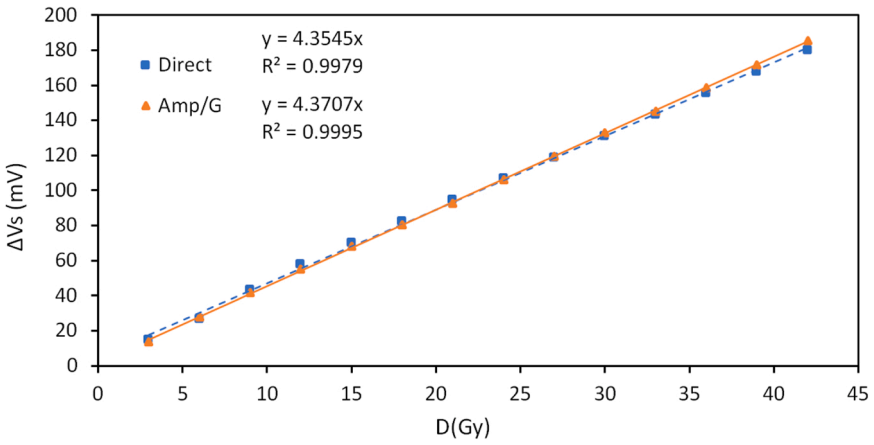

Fig. 4. Accumulated source voltage shift as a function of the measured dose. Data bar errors are smaller than symbols.

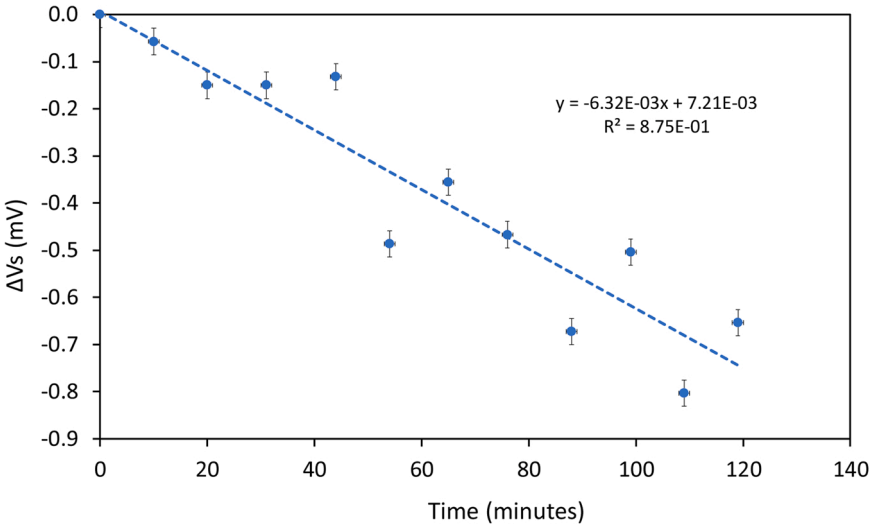

Fig. 5. Recovery of the source voltage after irradiation after an irradiation of 9 Gy.

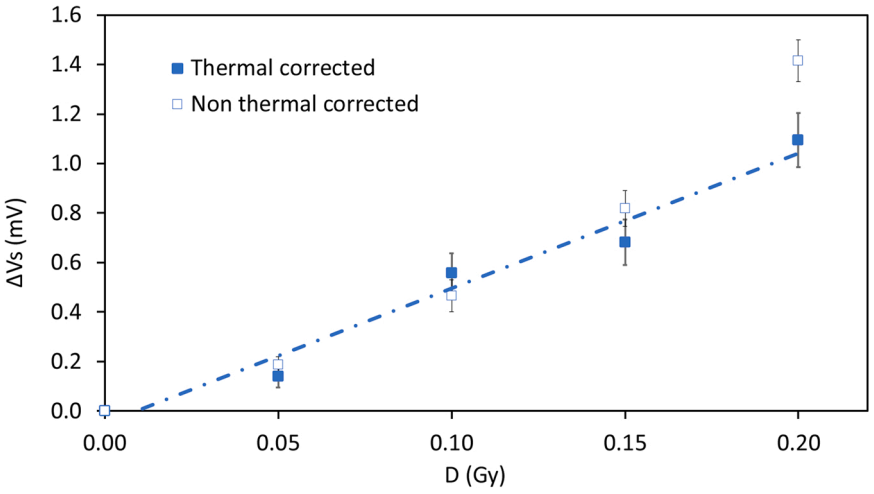

Fig. 6. Accumulated source voltage shift as a function of the absorbed dose obtained in low-dose experiments: data without thermal correction (empty symbols), and data with thermal correction (solid symbols). Dashed line shows the linear fit of the data with thermal correction.

4. Conclusions

A battery-less and wireless dosimetric system composed of an NFC tag with a pMOSFET-based dosimeter, a smartphone as the reader unit, and a cloud service based on MQTT protocol has been developed and evaluated in hospital facilities with potential application in dosimetry

Table 1
Improvements and/or novelties of the presented DosiTag system over the previous NFC-based dosimeter.

Feature	Previous NFC dosimeter [7]	DosiTag	Improvement/novelty
Circuit architecture	Only NFC chip	MCU + NFC chip	Inclusion of MCU allows the full control of the measurement variables (time, start/end, etc.)
NFC chip model	SL13A (AMS)	M24LR64E (STMicroelectronics)	The SL13A chip is a discontinued device
Sensitivity	4.75 ± 0.15 mV/Gy	4.37 ± 0.04 mV/Gy	Although average sensitivity has slightly been reduced, its associated uncertainty has been significantly reduced
Resolution	17 cGy	2 cGy	Resolution has improved by a factor of 8
Total dose	20 Gy	42 Gy	Total irradiation dose has been increased
Smartphone	Rooting required	No need to root	No root access is needed in the smartphone
Smartphone app	Designed for Android 5.1	Designed for Android 10	Smartphone app has been redesigned and improved. Higher Android versions are supported
IoT capabilities	No IoT implemented	Cloud service (based on MQTT protocol)	Integration with IoT allows classification, distribution and storage of patient's data
Irradiation area	Only sensor module	Whole tag	New version allows the irradiation of the complete dosimeter tag, not only the sensor module
Tag encapsulation	Not possible	Possible	Previous sensor connector made tag encapsulation impossible to be sterilized or submerged in liquids
Holder structure	Ad-hoc wood structure	No structure/holder is required	Previous version required a holder structure to ensure adequate and repeatable energy harvesting

control of radiotherapy treatments. This DosiTag system is based on a previous NFC dosimeter that has been redesigned and improved in several aspects. In particular, the system resolution has been improved by a factor of 8 thanks to the use of an instrumentation amplifier. Moreover, the thermal drift has been further reduced using a commercial bipolar buffer, obtaining a reduction of the thermal coefficient by 82 %. The measurement process, data storage and cloud publication are conducted through a custom-developed smartphone application. The inclusion of the MQTT broker to upload the measured data enables the classification of the dosimetry data and the identification of the NFC reader unit used for each patient, thus allowing a personalized follow-up and individual control of the patients. The integration of the sensor module on the PCB allows the board to be encapsulated and sterilized. The dosimetric characterization was conducted using a LINAC in hospital facilities, obtaining a sensitivity of (4.35 ± 0.17) mV/Gy for the low resolution channel and (4.37 ± 0.04) mV/Gy for the high resolution channel. The resolution of the LRC and HRC was 79 cGy and 2 cGy. The results are in good agreement with previous works and the system is still accurate after high radiation doses despite the entire area of the tag is irradiated. In conclusion, the achieved improved features of the developed DosiTag system support its potential use for clinical dose measurement in radiotherapy treatments.

CRediT authorship contribution statement

Pousibet-Garrido: Prototyping, experimentation, Writing – review & editing. **P. Escobedo:** Prototyping, Experimentation, reviewing and editing. **D. Guirado:** Experimentation, reviewing and editing, Data curation, Formal analysis, Methodology. **G.S. Ristic:** Writing – review & editing, Formal analysis. **A.J. Palma:** Conceptualization, Methodology, Writing – review & editing, Supervision. **M.A. Carvajal:** Conceptualization and data analysis, Investigation, Writing – review & editing, Supervision.

Declaration of Competing Interest

The authors declare that they have no known competing financial interests or personal relationships that could have appeared to influence the work reported in this paper.

Data availability

Data will be made available on request.

Acknowledgements

This research has been partially funded by Junta de Andalucía (Spain), projects numbers PI-0505–2017 FEDER/Junta de Andalucía-Consejería de Economía y Conocimiento Project B-TIC-468-UGR18, Proyecto del Plan Nacional I + D: PID2019–104888GB-I00 and Proyectos I + D + i Junta de Andalucía 2018: P18-RT-3237. This work was also conducted in the framework of H2020 ELICSIR project (grant No. 857558). P. Escobedo thanks grant IJC2020-043307-I funded by MCIN/AEI/ 10.13039/501100011033 and by "European Union Next-GenerationEU/PRTR".

References

[1] Development of Procedures for In Vivo Dosimetry in Radiotherapy, (2016). https://www.iaea.org/publications/8962/development-of-procedures-for-in-vivo-dosimetry-in-radiotherapy. (Accessed 28 September 2022).
[2] World Health Organization, F.R. of Institut für Strahlenhygiene des Bundesgesundheitsamtes (Germany), Quality assurance in radiotherapy: a guide prepared following a workshop held at Schloss Reisensburg, Federal Republic of Germany, 3–7 December 1984, World Health Organization, 1988. https://apps.who.int/iris/handle/10665/40423. (Accessed 28 September 2022).
[3] T. Kron, J. Lehmann, P.B. Greer, Dosimetry of ionising radiation in modern radiation oncology, Phys. Med Biol. 61 (2016) R167–R205, https://doi.org/10.1088/0031-9155/61/14/R167.
[4] L.L. Gunderson, J.E. Tepper, J.A. Bogart, eds., Clinical Radiation Oncology, fourth ed., Elsevier, Philadelphia, PA, 2016. https://www.clinicalkey.com/#!/browse/book/3-s2.0-C20130006482. (Accessed 28 September 2022).
[5] Best Medical Canada Products - MobileMOSFET, (n.d.). http://www.bestmedicalcanada.com/product_mobilemos.html. (Accessed 28 September 2022).
[6] A. Rozenfeld, Radiation Sensor and Dosimeter, US8742357B2, 2014. https://patents.google.com/patent/US8742357B2/en. (Accessed 28 September 2022).
[7] M.A. Carvajal, P. Escobedo, M. Jiménez-Melguizo, M.S. Martínez-García, F. Martínez-Martí, A. Martínez-Olmos, A.J. Palma, A compact dosimetric system for MOSFETs based on passive NFC tag and smartphone, Sens. Actuators A Phys. 267 (2017) 82–89, https://doi.org/10.1016/j.sna.2017.10.015.
[8] S. Alshaikh, M. Carolan, M. Petasecca, M. Lerch, P. Metcalfe, A. Rosenfeld, Direct and pulsed current annealing of p-MOSFET based dosimeter: the "MOSkin, Austral Phys. Eng. Sci. Med. 37 (2014) 311–319, https://doi.org/10.1007/s13246-014-0261-1.
[9] M.A. Garcia Inza, S.H. Carbonetto, J. Lipovetzky, A.N. Faigon, Radiation Sensor Based on MOSFETs Mismatch Amplification for Radiotherapy Applications, (2016). doi: 10.1109/TNS.2016.2560172.
[10] A. Holmes-Siedle, L. Adams, RADFET: a review of the use of metal-oxide-silicon devices as integrating dosimeters, Int. J. Radiat. Appl. Instrum. Part C Radiat. Phys. Chem. 28 (1986) 235–244, https://doi.org/10.1016/1359-0197(86)90134-7.
[11] A. Kelleher, W. Lane, L. Adams, A design solution to increasing the sensitivity of pMOS dosimeters: the stacked RADFET approach, IEEE Trans. Nucl. Sci. 42 (1995) 48–51, https://doi.org/10.1109/23.364881.
[12] R.A. Price, C. Benson, K. Rodgers, Development of a RadFET linear array for intracavitary in vivo dosimetry in external beam radiotherapy and brachytherapy, in: 2003 IEEE Nuclear Science Symposium. Conference Record (IEEE Cat. No.03CH37515), 3, 2003, 1494–1498. https://doi.org/10.1109/NSSMIC.2003.1352160.

[13] M.S. Martínez-García, J.T. del Río, A. Jaksic, J. Banqueri, M.A. Carvajal, Response to ionizing radiation of different biased and stacked pMOS structures, Sens. Actuators A Phys. 252 (2016) 67–75, https://doi.org/10.1016/j.sna.2016.11.007.
[14] C. Ehringfeld, S. Schmid, K. Poljanc, C. Kirisits, H. Aiginger, D. Georg, Application of commercial MOSFET detectors for in vivo dosimetry in the therapeutic x-ray range from 80 kV to 250 kV, Phys. Med. Biol. 50 (2005) 289–303, https://doi.org/10.1088/0031-9155/50/2/008.
[15] J.N. Roshau, D.E. Hintenlang, Characterization of the angular response of an "isotropic" MOSFET dosimeter, Health Phys. 84 (2003) 376–379, https://doi.org/10.1097/00004032-200303000-00012.
[16] H.A. Farroh, A. Nasr, K.A. Sharshar, A study of the performance of an N-Channel MOSFET under gamma radiation as a dosimeter, J. Electron. Mater. 49 (2020) 5762–5772, https://doi.org/10.1007/s11664-020-08330-4.
[17] G. Bharanidharan, D. Manigandan, K. Devan, V. Subramani, N. Gopishankar, T. Ganesh, R. Joshi, G. Rath, J. Velmurugan, P. Aruna, S. Ganesan, Characterization of responses and comparison of calibration factor for commercial MOSFET detectors, Med. Dosim. 30 (2005) 213–218, https://doi.org/10.1016/j.meddos.2005.08.004.
[18] O.F. Siebel, J.G. Pereira, M.C. Schneider, C. Galup-Montoro, A MOSFET dosimeter built on an off-the-shelf component for in vivo radiotherapy applications, in: Proceedings of the Fifth Latin American Symposium on Circuits and Systems, IEEE, 2014, 1–4. https://doi.org/10.1109/LASCAS.2014.6820261.
[19] V.V. Prikhodko, A.S. Alexeyev, P.A. Guskov, S.G. Novikov, A.I. Somov, V. V. Svetukhin, Technical note: ID-card-size dosimeter based on radiochromic films for continuous personnel monitoring, Med. Phys. 48 (2021) 3216–3222, https://doi.org/10.1002/mp.14893.
[20] Passive radiofrequency x-ray dosimeter tag based on flexible radiation-sensitive oxide field-effect transistor, Science Advances, (n.d.). https://www.science.org/doi/10.1126/sciadv.aat1825. (Accessed 30 September 2022).
[21] A.S. Beddar, M. Salehpour, T.M. Briere, H. Hamidian, M.T. Gillin, Preliminary evaluation of implantable MOSFET radiation dosimeters, Phys. Med. Biol. 50 (2005) 141–149, https://doi.org/10.1088/0031-9155/50/1/011.
[22] F. Li, Y. Bao, D. Wang, W. Wang, L. Niu, Smartphones for sensing, Sci. Bull. 61 (2016) 190–201, https://doi.org/10.1007/s11434-015-0954-1.
[23] V. Coskun, B. Ozdenizci, K. Ok, A survey on near field communication (NFC) technology, Wirel. Pers. Commun. 71 (2013) 2259–2294, https://doi.org/10.1007/s11277-012-0935-5.
[24] P. Teengam, W. Siangproh, S. Tontisirin, A. Jiraseree-amornkun, N. Chuaypen, P. Tangkijvanich, C.S. Henry, N. Ngamrojanavanich, O. Chailapakul, NFC-enabling smartphone-based portable amperometric immunosensor for hepatitis B virus detection, Sens. Actuators B Chem. 326 (2021), 128825, https://doi.org/10.1016/j.snb.2020.128825.
[25] P. Escobedo, M.D. Fernández-Ramos, N. López-Ruiz, O. Moyano-Rodríguez, A. Martínez-Olmos, I.M. Pérez de Vargas-Sansalvador, M.A. Carvajal, L.F. Capitán-Vallvey, A.J. Palma, Smart facemask for wireless CO_2 monitoring, Nat. Commun. 13 (2022) 72, https://doi.org/10.1038/s41467-021-27733-3.
[26] M. Boada, A. Lazaro, R. Villarino, D. Girbau, Battery-less NFC sensor for pH monitoring, IEEE Access 7 (2019) 33226–33239, https://doi.org/10.1109/ACCESS.2019.2904109.
[27] A. Lazaro, M. Boada, R. Villarino, D. Girbau, Color measurement and analysis of fruit with a battery-less NFC sensor, Sensors 19 (2019) 1741, https://doi.org/10.3390/s19071741.
[28] A compact and low cost dosimetry system based on MOSFET for in vivo radiotherapy, Elsevier Enhanced Reader, (n.d.). https://doi.org/10.1016/j.sna.2012.05.024.
[29] M. Garcia-Inza, M. Cassani, S. Carbonetto, M. Casal, E. Redín, A. Faigón, 6MV LINAC characterization of a MOSFET dosimeter fabricated in a CMOS process, Radiat. Meas. 117 (2018) 63–69, https://doi.org/10.1016/j.radmeas.2018.07.009.
[30] D. Dinculeană, X. Cheng, Vulnerabilities and limitations of MQTT protocol used between IoT devices, Appl. Sci. 9 (2019) 848, https://doi.org/10.3390/app9050848.
[31] D. Soni, A. Makwana, A survey on MQTT: a protocol of internet of things (IOT), in: Proceedings of the International Conference on Telecommunication, Power Analysis and Computing Techniques (ICTPACT-2017), 20, 173–177.
[32] R.A. Atmoko, R. Riantini, M.K. Hasin, IoT real time data acquisition using MQTT protocol, J. Phys. Conf. Ser., 853 (2017) 012003. https://doi.org/10.1088/1742–6596/853/1/012003.
[33] H.C. Hwang, J. Park, J.G. Shon, Design and implementation of a reliable message transmission system based on MQTT protocol in IoT, Wirel. Pers. Commun. 91 (2016) 1765–1777, https://doi.org/10.1007/s11277-016-3398-2.
[34] M.A. Carvajal, M.S. Martínez-García, D. Guirado, J. Banqueri, A.J. Palma, Dose verification system based on MOS transistor for real-time measurement, Sens. Actuators A Phys. 247 (2016) 269–276, https://doi.org/10.1016/j.sna.2016.06.009.
[35] N.D. Vasović, G.S. Ristić, A new microcontroller-based RADFET dosimeter reader, Radiat. Meas. 47 (2012) 272–276, https://doi.org/10.1016/j.radmeas.2012.01.017.
[36] O.F. Siebel, J.G. Pereira, R.S. Souza, F.J. Ramirez-Fernandez, M.C. Schneider, C. Galup-Montoro, A very-low-cost dosimeter based on the off-the-shelf CD4007 MOSFET array for in vivo radiotherapy applications, Radiat. Meas. 75 (2015) 53–63, https://doi.org/10.1016/j.radmeas.2015.03.004.
[37] A. Kelleher, M. O'Sullivan, J. Ryan, B. O'Neill, W. Lane, Development of the radiation sensitivity of PMOS dosimeters, IEEE Trans. Nucl. Sci. 39 (1992) 342–346, https://doi.org/10.1109/23.277514.
[38] J.R. Schwank, S.B. Roeske, D.E. Beutler, D.J. Moreno, M.R. Shaneyfelt, A dose rate independent pMOS dosimeter for space applications, IEEE Trans. Nucl. Sci. 43 (1996) 2671–2678, https://doi.org/10.1109/23.556852.
[39] M24LR64E-R - Dynamic NFC/RFID tag IC with 64-Kbit EEPROM, Energy Harvesting, I2C bus and ISO 15693 RF Interface - STMicroelectronics, (n.d.). https://www.st.com/en/nfc/m24lr64e-r.html. (Accessed 28 September 2022).
[40] M.A. Carvajal, M.S. Martínez-García, D. Guirado, A. Martínez-Olmos, A.J. Palma, Thermal compensation technique using the parasitic diode for DMOS transistors, Sens. Actuators A Phys. 249 (2016) 249–255, https://doi.org/10.1016/j.sna.2016.09.004.
[41] B. Eslami, S. Ashrafi, Effect of gamma ray absorbed dose on the FET transistor parameters, Results Phys. 6 (2016) 396–400, https://doi.org/10.1016/j.rinp.2016.07.003.
[42] S.M. Pejovic, M.M. Pejovic, D. Stojanov, O. Ciraj-Bjelac, Sensitivity and fading of pMOS dosemeters irradiated with X-ray radiation doses from 1 to 100 cGy, Radiat. Prot. Dosim. 168 (2016) 33–39, https://doi.org/10.1093/rpd/ncv006.

Antonio Pousibet-Garrido was born in La Carolina (Spain) in 1998. He received the B.S. degree in Telecommunication Engineering, and the M.Sc. degree in Industrial Electronics, both from the University of Granada (Granada, Spain) in 2021 and 2022, respectively. Since 2023, he is Ph.D. student of Information and Communication Technologies at the University of Granada. His research interests include NFC-based sensorized systems, and dosimetry-related studies.

Pablo Escobedo Araque was born in Jaén (Spain) in 1989. He received the Major degrees in Telecommunication Engineering and Electronics Engineering from the University of Granada (Granada, Spain) in 2012 and 2013, respectively, and the Master's degree in Computer and Network Engineering in 2014. In 2018, he received his Ph.D. degree in design and development of printed sensor systems on flexible substrates at the same Institution. He is currently a postdoctoral researcher at the ECSens Group (Department of Electronics and Computer Technology, University of Granada). His research interests include the development of printed sensor systems on flexible substrates, including RFID/NFC tags with sensing capabilities, for applications in multiple fields such as environmental monitoring, clinical and health analysis/diagnosis, smart packaging of goods and food, and wearable systems for sports activity and biomedical monitoring.

Damián Guirado Llorente was born in Murcia (Spain) in 1967, obtained his MSc degree in Physics in 1993 and his Ph.D. degree in 2012 both at the University of Granada (Spain). He works at the San Cecilio University Hospital in Granada as medical physics specialist, and he has combined his clinical activity, as a healthcare specialist, with research activity; developing his professional career at the same time he has participated in several research projects with an orientation according to this circumstance: the clinical application of their results. He is interested in various topics related to medical physics, such as ionizing radiation dosimetry and metrology, radiation therapy and radiobiology.

Goran Ristic was born on August 2, 1964 in Niš, Serbia. He received the B.Sc. degree in physics, and the M.Sc. and Ph.D. degrees in electronics at University of Niš, Serbia, in 1990, 1994 and 1998. He is a Full Professor and Head of Applied Physics Laboratory at the Faculty of Electronic Engineering, University of Niš. His research includes radiation dosimeters, the reliability of MOS transistor (the radiation and post-irradiation effects, as well as the electrical and post-electrical stress effects), the electrical discharge and recombination processes in the afterglow periods in gases, and medical X-ray imaging. He is is author or co-author of more than 100 research papers, including 80 papers in journals from WoS list. On the basis of SCOPUS data, his papers have been cited more than 1500 times (excluding self citations), and his H – index is 18 (excluding self citations).

Alberto J. Palma is full Professor of Electronic Technology at the University of Granada, received his M.Sc. in Physics (1991) and Ph.D. in Physics (1995) from the Faculty of Sciences, University of Granada (Spain). Since 1992, he has been working on trapping of carriers in different electronic devices (diodes and MOS transistors) including characterization and simulation of capture cross sections, random telegraph noise, and generation-recombination noise in devices. He founded, together with Prof. Capitán-Vallvey, the interdisciplinary group ECsens, which includes Chemists, Physicists and Electrical and Computer Engineers at the University of Granada in 2000. His current research interests are the design, development and fabrication of sensors and portable instrumentation for environmental, health and food analysis and monitoring. He is also interested in printed sensors, flexible electronics and capillary-based microfluidic devices.

Miguel A. Carvajal Rodríguez was born in 1977 in Granada (Spain). He received the MSc degrees in Physics in 2000 and the MSc degree in Electronic Engineering in 2002, both from the University of Granada; and the Ph.D. degree in Electronic Engineering from the University of Granada in 2007 about the development a dosimeter system based on commercial MOSFETs. Currently he works as tenured Professor at the University of Granada. His research interests include the effects of irradiation and post-irradiation in MOSFET transistors, RFID tags with sensor capabilities, gas sensor and electrochemiluminescent sensors, and their applications to handheld instrumentation.